

# A Novel Optimization Method for the Electric Topology of Thermoelectric Modules Used in an Automobile Exhaust Thermoelectric Generator

RUI QUAN,<sup>1,3</sup> XINFENG TANG,<sup>1</sup> SHUHAI QUAN,<sup>2</sup> and LIANG HUANG<sup>2</sup>

1.—State Key Laboratory of Advanced Technology for Material Synthesis and Processing, Wuhan University of Technology, Wuhan, China. 2.—School of Automation, Wuhan University of Technology, Wuhan, China. 3.—e-mail: quan\_rui@126.com

Based on  $\text{Bi}_2\text{Te}_3$  thermoelectric modules, a kind of automobile exhaust thermoelectric generator (AETEG) with a single-column cold-source structure was designed. To enhance its net power and efficiency, the output performance of all the thermoelectric modules was tested with a temperature monitoring unit and voltage monitoring unit, and modeled using a back-propagation (BP) neural network based on various hot-source temperatures, cold-source temperatures, load currents, and contact pressures according to the temperature distribution of the designed heat exchanger and cooling system. Then, their electric topology (series or parallel hybrid) was optimized using a genetic algorithm to achieve the maximum peak power of the AETEG. From the experimental results, compared with when all the thermoelectric modules were connected only in series or parallel at random, it is concluded that the AETEG performance is evidently affected by the electric topology of all the single thermoelectric modules. The optimized AETEG output power is greatly superior to the other two investigated designs, validating the proposed optimized electric topology as both feasible and practical.

**Key words:** Thermoelectric modules, automobile exhaust thermoelectric generator, electric topology, genetic algorithm

## INTRODUCTION

The efficiency of traditional internal combustion engines is about 30%, while nearly 40% of the fossil energy is wasted directly through the exhaust or coolant.<sup>1</sup> Thus, recovery of exhaust heat energy via thermoelectric technology for use in the vehicle system is important and can significantly enhance both fuel economy and system performance. To achieve this goal, use of thermoelectric generators (TEGs) based on single, low- and intermediate-temperature thermoelectric modules has been a novel research focus. Some prototype serial TEGs with optimal net power  $W_e = 1$  kW for trucks and  $W_e = 0.2$  kW to 0.5 kW for cars are under development.<sup>2–4</sup>

The single thermoelectric module is a kind of advanced generator based on the Seebeck effect.<sup>5</sup> Its output performance is proportional to the temperature difference between its hot side and cold side. An AETEG usually includes many thermoelectric modules with different characteristics and temperature distributions according to their location between the heat exchanger and cooling system, and their electric topology (series or parallel) directly affects the overall output performance. Thus, it is essential to optimize the electric topology according to the characteristics of each thermoelectric module and the temperature distributions of the heat exchanger and cooling system.

## DESIGN OF THE AETEG

A schematic of the designed AETEG is shown in Fig. 1. In our experimental setup there is an

(Received July 5, 2012; accepted September 25, 2012; published online October 27, 2012)

independent cooling system which includes a water box, pump, fan, valve 1, and valve 2. There are one heat exchanger, two cooling units, and two groups of thermoelectric modules. For the thermoelectric modules of each layer, all the hot sides are connected with the heat exchanger, while their cold sides are connected with cooling units 1 and 2, respectively. The operating parameters such as the overall voltage and current of the AETEG are detected by the main controller with a 12-bit analog-to-digital (A/D) module and monitored by a PC-based software interface. Moreover, the actuators such as valve 1, valve 2, pump, fan, relay S1, etc. are controlled by the main controller through an input/output (I/O) module. In addition, the thermoelectric modules of each group distributed above the heat exchanger are arranged in four rows and eight columns as shown in Figs. 2 and 3, respectively.

Cooling units 1 and 2 form the single-column cold-source structure; i.e., the cold sides of the four thermoelectric modules of each column in a layer are fixed with a common small cooling box, whereas

the eight cooling boxes of each layer compose the whole cooling unit. The specific cooling unit structure is presented in Fig. 4; the contact pressure among the thermoelectric modules, heat exchanger, and cooling units can be adjusted arbitrarily.

There are a series of dummy plates at both sides of the heat exchanger's interior cavity, here called the herring-bone structure. The effective heat conduction length is 400 mm, the effective width is 280 mm, the exterior height is 18 mm, the interior thickness is 2 mm, and the dimensions of all the parts of the heat exchanger are given in Fig. 5.<sup>6</sup>

### PARAMETERS OF AETEG

The engine adopted in the designed AETEG is made by Citroën of France (PSA RFN 10LH3X). The heat exchanger is made of brass, and all the thermoelectric modules are manufactured from Bi<sub>2</sub>Te<sub>3</sub> materials for use at low operating temperature. The specific parameters of the relevant components of the AETEG are listed in Table I.

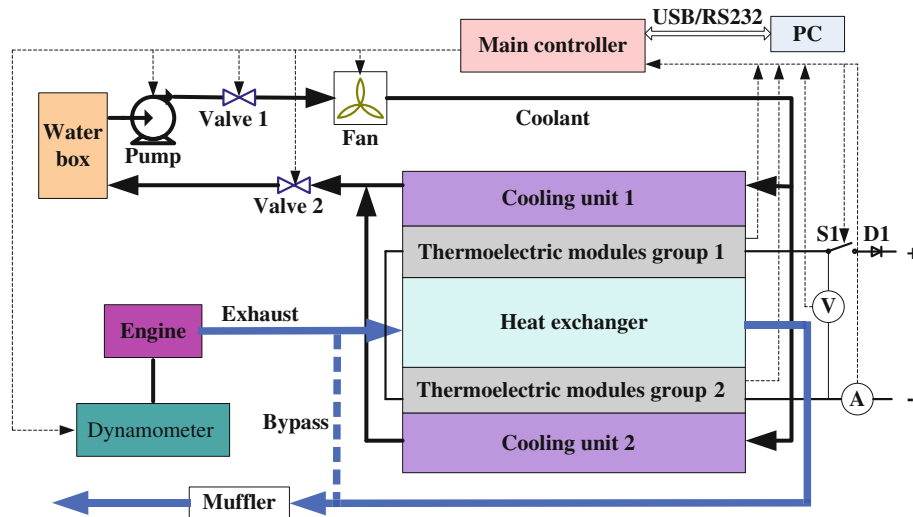


Fig. 1. Schematic of the designed AETEG.

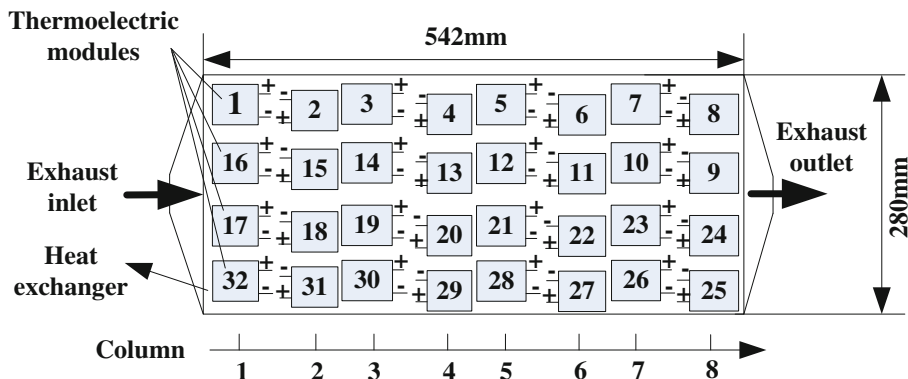


Fig. 2. Number and distribution of thermoelectric modules in group 1.

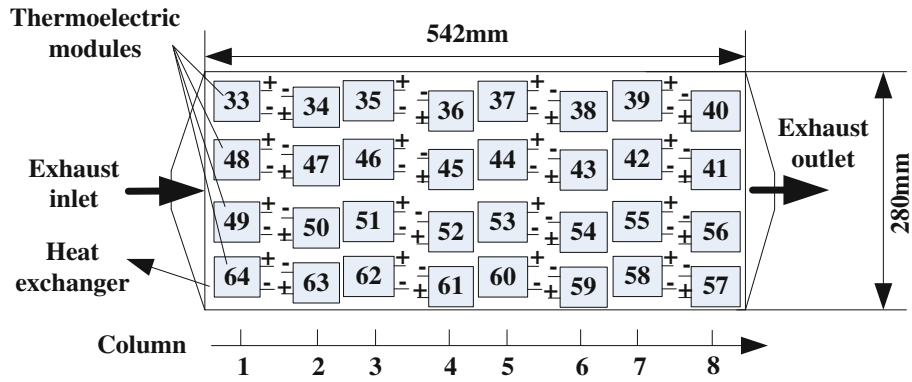


Fig. 3. Number and distribution of thermoelectric modules in group 2.

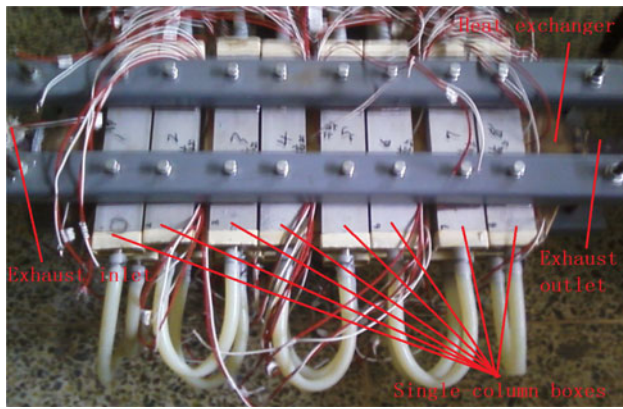


Fig. 4. Cooling unit with a single column of boxes.

### VOLTAGE MONITORING UNIT AND TEMPERATURE MONITORING UNIT OF AETEG

To detect and analyze the voltage of the 64 single thermoelectric modules used in the AETEG with different temperature differences, contact pressures, output currents, etc., a voltage monitoring unit and a temperature monitoring unit were designed for use in the experiment. When the AETEG is applied in a vehicle electric system these are not essential and can be omitted to simplify the system.

The voltage monitoring unit includes four slave monitoring boards, each of which can detect the real-time voltage of 16 single thermoelectric modules. All the slave monitoring boards communicate with the main controller via an interior controller area network (CAN) bus.<sup>7</sup> As shown in Fig. 2, the hot-source and cold-source temperatures of the thermoelectric modules must be monitored for optimization of their electric topology. All four thermoelectric modules in each column above the heat exchanger share a common box, and the surface temperature of each single-column box can be taken as their cold-source temperature. Thus, 40 channel temperatures should be monitored in each

layer, and 80 temperature monitoring channels were designed for the symmetrical interior structure of the heat exchanger; i.e., 32 temperature detection points are selected above the surface of the heat exchanger, and 8 corresponding temperature detection points are selected below the surface of the 8 single-column boxes. Eight slave temperature monitoring boards were designed, each of which can detect 11 temperature channels; they also communicate with the main controller via an interior CAN bus.<sup>8</sup>

### OPTIMIZATION OF ELECTRIC TOPOLOGY

Due to the different voltage and current characteristics of each thermoelectric module, if they are all connected in series, the output current of the AETEG is restricted by the one with the minimum temperature difference; i.e., the voltage of several thermoelectric modules will be close to zero or negative once the load current increases to some degree. In contrast, if a number of modules with different open-voltage values are connected in parallel, there will be a ring current among them, as their final output voltage has to be the same, which will increase the internal power loss.<sup>9</sup> For a single thermoelectric module with a certain applied temperature difference, the current corresponding to the peak power (denoted  $I_p$ ) is different from the current corresponding to its maximum efficiency (denoted  $I_e$ ). Thus, to optimize the electric topology of all the thermoelectric modules of the AETEG in Fig. 1, the peak power of the AETEG should be the largest with current of  $I_p$  when all the temperatures are steady and the operation condition is constant, i.e., when all the single thermoelectric modules are, as far as possible, operating in the range between their maximum power and maximum efficiency. The total internal resistance (denoted  $r$ ) of each thermoelectric module is calculated from Eq. 1.

$$r = l_p / (\sigma_p A_p) + l_n (\sigma_n A_n), \quad (1)$$

where  $\sigma_p$  and  $\sigma_n$  are the conductivities,  $l_p$  and  $l_n$  are the lengths, and  $A_p$  and  $A_n$  are the areas of the

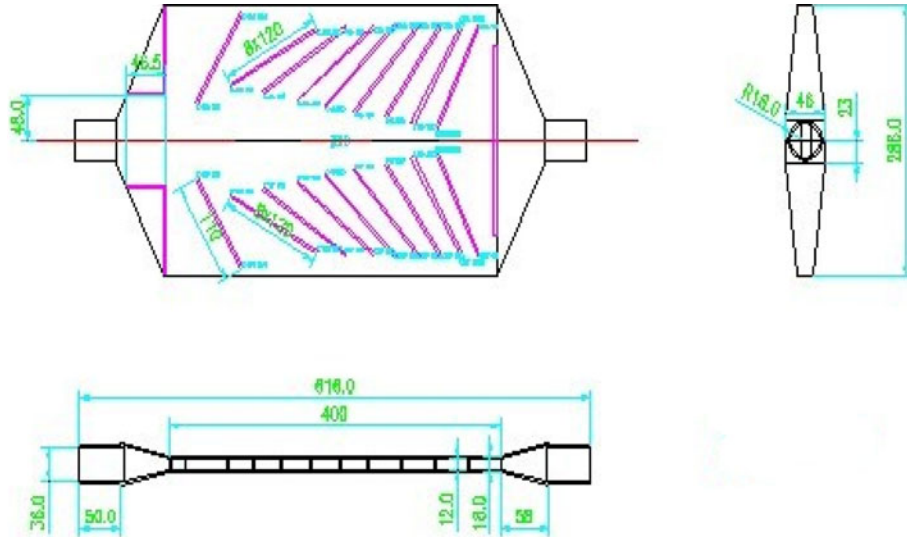


Fig. 5. Dimensions of the heat exchanger with herring-bone cavity.

**Table I. Parameters of relevant components of the AETEG**

Name	Parameter
Engine	Engine capacity: 1997 cc Maximum power: 108 kW (6000 r/min) Maximum torque: 200 NM (4000 r/min)
Dynamometer	Maximum absorbed power: 160 kW Maximum rotation speed: 6000 r/min Maximum absorbed torque: 600 NM
Pump	Power: 220 V <sub>AC</sub> Maximum power: 750 W Total displacement: 13200 kg/h
Fan	Power supply: 12 V <sub>DC</sub> Rated power: 750 W
Heat exchanger	Interior thickness: 3 mm Heat conduction area: 542 mm × 280 mm
Cooling box	Dimensions: 280 mm × 60 mm × 26 mm
Thermoelectric module	Maximum operating temperature: 350°C Dimensions: 56 mm × 56 mm × 6 mm

*p*- and *n*-type semiconductor of a single thermoelectric module, respectively. Even though the number of *p*-type and *n*-type semiconductor couples of each single thermoelectric module adopted in Fig. 1 is 128 and the parameters in Eq. 1 are the same, each thermoelectric module does not have the same total internal resistance due to their inconsistency and different contact pressures.

In our work, all the single thermoelectric modules with the same or similar open-circuit voltage value can be connected in parallel as a basic voltage element so that little ring current exists among them. Then, all the different basic voltage elements are connected in series to form the overall AETEG. Once the output power of the AETEG reaches its peak value as the load current increases (i.e., the load resistance is almost equal to the total internal

resistance of the AETEG), all the corresponding  $I_p$  values of each basic voltage element should be almost the same so that all the single thermoelectric modules work normally and efficiently.

Firstly, all the single thermoelectric modules were modeled using a three-layer BP neural network, taking into account parameters such as the hot-source temperature ( $T_H$ ), cold-source temperature ( $T_L$ ), contact pressure ( $F$ ), output current ( $I$ ), and output voltage ( $U$ ). The model used for each single thermoelectric module is presented in Fig. 6.  $T_H$ ,  $T_L$ ,  $F$ , and  $I$  are the input variables, the output variable is  $U$ , the hidden function selected is tansig, and the training goal is 0.001. The output layer function is logsig, and considering Kolmogorov theorem, the hidden layer number is 6. Based on the voltage monitoring unit and temperature monitoring unit,

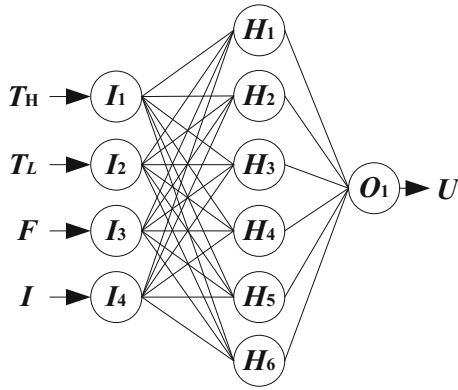


Fig. 6. BP neural network model of each single thermoelectric module.

combined with the testbench data for different  $F$ ,  $I$ , and  $U$  values, 300 different datasets for  $T_H$ ,  $T_L$ ,  $F$ ,  $I$ , and  $U$  were selected to train the BP neural network of each single thermoelectric module using the Levenberg–Marquardt (LM) algorithm.<sup>10</sup>

Then, based on the models established above, the electric topology of all the single modules was optimized using a genetic algorithm (GA).<sup>11</sup> The objective function used was the maximum peak power of the AETEG ( $P_{\max}$ ), described by Eq. 2.

$$P_{\max} = f(T_{Hi}, T_{Li}, F_i, I_i) \quad (i = 1, 2, \dots, 64). \quad (2)$$

The constraints are

$$T_{Hi} \leq T_{\max}(H) \quad (i = 1, 2, \dots, 64), \quad (3)$$

$$T_{Li} \leq T_{\max}(L) \quad (i = 1, 2, \dots, 64), \quad (4)$$

$$F_i \leq F_{\max} \quad (i = 1, 2, \dots, 64), \quad (5)$$

$$I_i \leq I_{\max} \quad (i = 1, 2, \dots, 64), \quad (6)$$

where  $T_{\max}(H)$ ,  $T_{\max}(L)$ ,  $F_{\max}$ , and  $I_{\max}$  are the maximum hot-source temperature, maximum cold-source temperature, maximum contact pressure, and maximum output current (i.e., short-circuit current) of a single thermoelectric module, respectively.

Based on C++ language, an optimization program was designed; the program flowchart is shown in Fig. 7, and the optimized parameters of the genetic algorithm were as follows: the colony number is 128, the crossover probability is 0.6, the variation probability is 0.01, and the termination generation number is 200.

## EXPERIMENTAL RESULTS AND DISCUSSION

To analyze the effect of the electric topology as optimized by the GA in our work, the output performance of the AETEG with three different kinds of electric topology is compared in this section. In

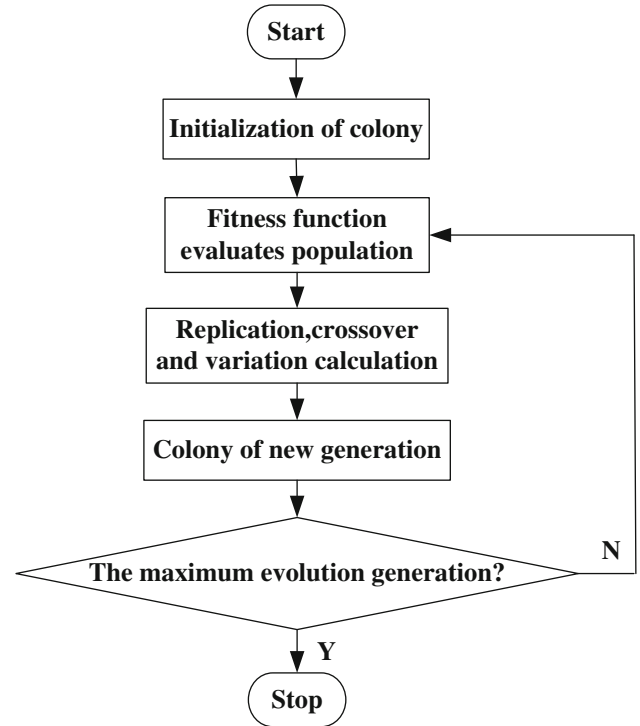


Fig. 7. Program flowchart of the genetic algorithm.

the first case, all the single thermoelectric modules used in the AETEG were connected in series. In the second case, the single thermoelectric modules of each column are first connected in series, then those in the same column in both thermoelectric module group 1 and 2 are connected in parallel as an unit, then each unit is connected in series as the overall output of the AETEG; we call this the parallel hybrid electric topology, as shown in Fig. 8. Figure 9 shows the third and final electric topology of the AETEG as optimized by the GA based on the optimization method stated above, where several single thermoelectric modules of lower performance but similar electric characteristics are connected in parallel, while the others with superior performance and similar  $I_p$  values are connected in series accordingly.

Due to the nonuniform temperature distribution of the hot-source spots corresponding to each thermoelectric module, once the maximum temperature approaches the maximum operating temperature (350°C), the exhaust from the engine is bypassed in order to protect the corresponding thermoelectric module. Figure 10 depicts the voltage–current–power ( $V$ – $I$ – $P$ ) characteristics of the three different electric topologies presented above when their maximum hot-source temperature is 350°C. As the current increases, their voltage decreases accordingly with almost the same slope, while the power first increases to a peak value then reduces; thus, the output characteristic of the AETEG is extremely soft, regardless of the electric topology applied. It is

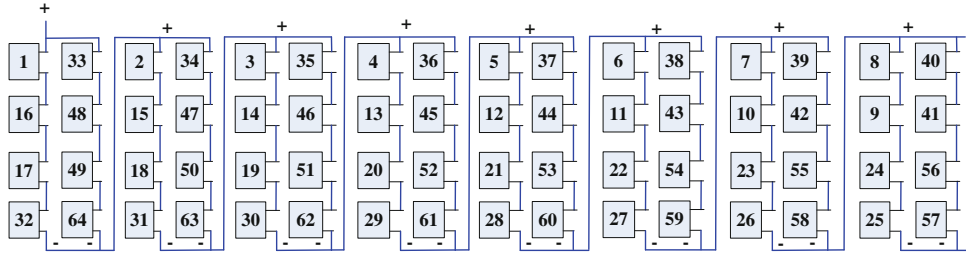


Fig. 8. Parallel hybrid AETEG electric topology.

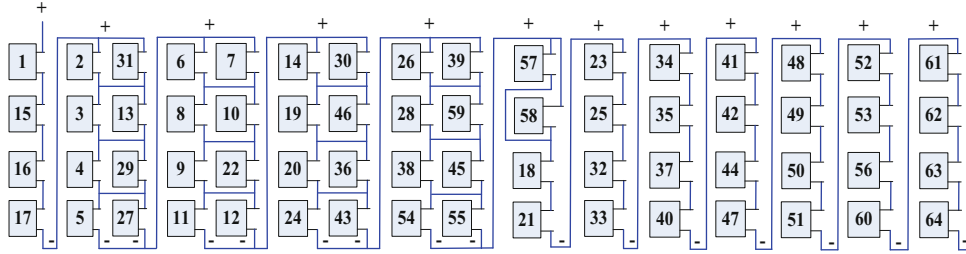


Fig. 9. Electric topology of the AETEG as optimized by the GA.

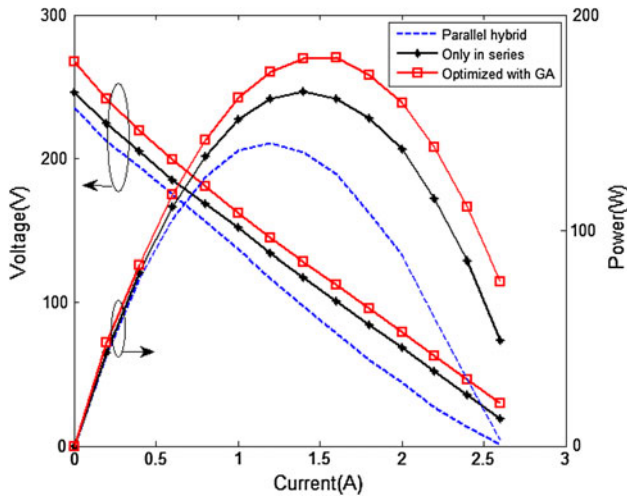


Fig. 10.  $V-I-P$  characteristics for maximum hot-source temperature of 350°C.

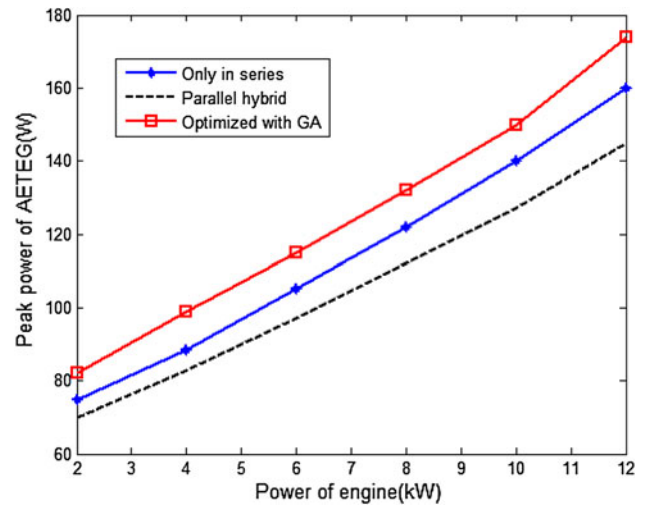


Fig. 11. Maximum power of the AETEG in different electric topologies as a function of engine power.

evident that the voltage and power of the AETEG as optimized by the GA are the highest for the same load current, while the voltage and power of the AETEG with the parallel hybrid electric topology are the lowest under this condition. The peak power of the AETEG as optimized by the GA and in the series and parallel hybrid topologies is 179 W, 164 W, and 141 W, respectively. It can easily be seen that the performance of the AETEG is related to its electric topology, with the electric topology as optimized in our work showing improved AETEG performance.

For different engine output powers (with engine rotation speed increasing from 2500 r/min to

3200 r/min), and corresponding different maximum hot-source temperatures, the method described above was used to determine the peak AETEG power for the described engine operation conditions using the three different electric topologies of the AETEG. The results are shown in Fig. 11, which demonstrates that the peak AETEG power as optimized in this work is much larger than that obtained in the parallel hybrid or series topologies. The electric topology as optimized by the GA is enhanced by about 10% compared with the series topology, showing that the optimized topology is both feasible and practical.

## CONCLUSIONS

Automotive waste heat recovery based on thermoelectric modules represents a promising research focus worldwide, but enhancement of AETEG performance with current thermoelectric modules remains a significant challenge.  $\text{Bi}_2\text{Te}_3$  is the most common commercially available material used in TEG modules to date. Despite the high  $ZT$  value of about 1.1 offered by this material, it has a very restrictive operating temperature range (usually  $20^\circ\text{C}$  to  $300^\circ\text{C}$ ) and relatively large thermal resistance. Also, it is not technically possible to greatly enhance the performance of TEG modules only by increasing the  $ZT$  value (e.g., to above 3) of the  $\text{Bi}_2\text{Te}_3$  material at present, focusing effort on increasing the peak AETEG power through optimization of its electric topology, taking into account the heat transfer mechanisms for various subsystems such as the heat exchanger and cooling units. From the presented comparisons of the peak power obtained with three different electric topologies, we find that the AETEG performance is evidently affected by its electric topology for given conditions, and the topology optimized by the GA in our work presents obvious advantages over the series or parallel hybrid topologies.

A useful approach is to change the input exhaust gas temperature and flow rate in order to increase the temperature difference across the AETEG once its cooling system has been determined. However, the change in the gas flow rate caused by the heat exchanger may degrade the performance of the engine, such as its emission behavior, dynamic properties, and fuel economy. Thus, it is important to optimize the structure of the heat exchanger and muffler without greatly altering the gas flow. In our work, a heat exchanger with a herring-bone cavity was adopted, as it can recover exhaust heat efficiently without greatly increasing the back-pressure of the gas flow.

As shown in Fig. 10, due to the soft output characteristic of the AETEG, a direct current (DC)/DC

converter must be connected with the AETEG to interface its output to the vehicle's electric system. For different values of the engine output power, temperature difference, and peak AETEG power, the approach of maximum power point tracking (MPPT) using real-time control of the output and input currents of the DC/DC converter should be applied to charge the battery or supply power to the vehicle's electric system according to different driving cycles, in order to enhance the efficiency and performance of the AETEG.

## ACKNOWLEDGEMENTS

This work was partially supported by the National Program on Key Basic Research Project (973 Program) of China (Grant No. 2007CB607500) and the International Science and Technology Cooperation Program of China (Grant No. 2011DFB60150).

## REFERENCES

1. S. Kim, S. Park, S. Kim, and S.H. Rhi, *J. Electron. Mater.* 40, 5 (2011).
2. D.M. Rowe, *Proceedings of the XIIIth Forum on Thermoelectricity*, Report No. O3.1 (Kiev: Institute of Thermoelectricity, 2009).
3. Kh.M. Saqr, M.Kh. Mansour, and M.N. Musa, *J. Thermoelectr.* 1, 59 (2008).
4. H.T. Kaibe, I. Aoyama, and S. Sano, *J. Thermoelectr.* 1, 59 (2009).
5. A. Boyer and E. Cisse, *Mater. Sci. Eng. B Solid. State. Adv. Technol.* B13, 2 (1992).
6. R. Quan, X.F. Tang, S.H. Quan and L. Huang, *Proceedings of 2012 International Conference on Frontiers of Advanced Materials and Engineering Technology, IFSTRA* (2012), p. 1430.
7. R. Quan, X.F. Tang, S.H. Quan and L. Huang, *Proceedings of 2012 International Conference on Advanced Mechanical Engineering, ITIERS* (2012), in press.
8. Q. Hu, L. Huang and R. Quan, *J. Wuhan Univ. Technol. Inf. Manag. Eng.* 2, 32 (2011).
9. R. Quan, S.H. Quan, L. Huang, and X.F. Tang, *J. Shanghai Jiaotong Univ.* 45, 6 (2011).
10. L.S.H. Ngia and J.S. Jöberg, *IEEE Trans. Sig. Process.* 7, 48 (2000).
11. K. Suga, S. Kato, and K. Hiyama, *Build. Environ.* 5, 45 (2010).